Micro-machined ionic liquid electrospray thrusters for Cubesat applications

IEPC-2017-224

Presented at the 35th International Electric Propulsion Conference
Georgia Institute of Technology – Atlanta, Georgia – USA
October 8–12, 2017

David Krejci* and Paulo Lozano†
Massachusetts Institute of Technology, Cambridge, MA, 02139, USA

Micromachined electrospray thrusters have the potential to provide high performance propulsion for small satellites in an unmatched small packaging, featuring 480 emitter tips per square centimeter. This work presents the extended duration firing results of such ionic liquid electrospray thrusters with different propellant reservoir systems. These thrusters are comprised of a porous glass emitter array, packaged with an extractor electrode with individual apertures for each of the 480 emitter tips. The electrospray array is fed passively with the ionic liquid propellant from an attached reservoir by capillary action. Firing data from a test with total duration of > 300hr are presented, including stable emission > 100hr in open-loop mode. In addition, the firing data of a flight-ready thruster is presented, which shows the ability of these devices to completely deplete the ionic liquid stored in the reservoir. Two flight-ready thrusters were integrated with a to a Cubesat-comaptible power processing unit. In this test, both thrusters were able to deplete the stored propellant without premature failure. Thrust data is estimated based on emission current and propellant consumption, yielding $T \sim 14\mu$N per array, which is consistent with previous device characterizations. Potential application of this technology to Cubesats is discussed and resulting performance are discussed.

Nomenclature

I	Current, A
I_{sp}	Specific impulse, m/s
J	Impulse, Ns
m/q	Mass-to-charge ratio, C/kg
t	Time, s
T	Thrust, N
V	Potential, V
η	Efficiency, -

I. Introduction

The field of small satellites has experienced a dramatic growth in recent years with mission concepts involving the use of nano- and pico-satellites (such as 1 kg CubeSats and smaller) in diverse applications.[1,2,3] The development of miniaturized technologies coupled with limiting government budgets and a stronger involvement of the commercial sector have been important to support this trend. While microelectronics and many electromechanical and structural systems have been successfully incorporated in small satellites, adequate propulsion systems remain in a developmental stage. Propulsion would enable small satellites to

*Research Scientist, Department of Aeronautics and Astronautics, krejci@mit.edu.
†Professor, Department of Aeronautics and Astronautics, plozano@mit.edu.

perform the kind of tasks that larger systems already do, such as station keeping, attitude control and orbital changes, including de-orbit at the end of their operational life. At the same time, propulsion would be essential in advanced applications, like formation flying, constellation deployment and maintenance, space debris mitigation, and inspection and repair of valuable space assets.

Among several options considered for propulsion of small satellites, micro-fabricated electrospray thrusters are an attractive alternative due to their intrinsic small size and potential for high specific impulse and efficiency.[4,5,6,7,8,9,10,11,12,13] In these propulsion devices, ions and sometimes nanometer-sized charged droplets, are directly extracted from the surface of room-temperature molten salts, also known as ionic liquids (IL). The liquid is passively supplied to a sharp structure, or emitter, via capillary forces while a voltage is applied between the liquid in the emitter and an aperture electrode. When the electrostatic stress on the liquid surface overcomes surface tension, the liquid deforms into a sharp meniscus, thus amplifying the electric field to values in excess of 1 V/nm in a region measuring a few nanometers at the apex of the electrified meniscus. This large field induces the extraction and acceleration of molecular ions directly from the liquid surface, producing thrust.[14,15,16,17,18] Because of the composition of ionic liquids, such a device allows extraction of both positive and negative ions, therefore preventing satellite charge-up by firing a pair of thrusters with opposite polarity.[19]

Most of the mass and volume of electric propulsion ion engines used in large satellites are necessary to support gas ionization, making these engines challenging to miniaturize.[20] In contrast, there is no ionization volume in electrospray thrusters, thus allowing their construction in exceptionally small devices using micromechanical systems (MEMS) processes.[7,6,21,22,11,8] The thrust generated by a single emitter is on the order of 100 nN, which is too low to comply with typical satellite requirements. To overcome this limitation, arrays of large number of capillary and porous emitters have been proposed and developed, effectively multiplexing emission current and therefore thrust.[6,7,8,10]

Most of these developments have focused on the emitter fabrication and emission characteristics, but until now none have been operated for long enough to demonstrate propellant consumption from an unpressurized reservoir compatible with the space environment. When testing emitter arrays at constant voltage, various researchers have reported current traces that decrease monotonically with time reaching 10-50% of the original value in seconds to minutes.[23,24,7,11,6] While some of these decays could be attributed to the lack of a reservoir, their time characteristics are much shorter than the anticipated propellant consumption time. Significant effort has therefore been devoted to study the causes for decreased emission of current, identifying sources that act on different time scales ranging from minutes to thousands of hours.

Lozano and Martinez-Sanchez[4] showed that electrochemical degradation occurred when the voltage across the double layer between a metallic emitter and the liquid surpasses the electrochemical window limit for faradic reactions. They showed that alternating the polarity of the emitter potential could mitigate charge accumulation in the double layer and therefore prevent reactions. Expanding these findings, Brikner and Lozano[25] introduced the concept of a distal electrode in conjunction with a dielectric emitter material, thus removing the possibility of reactions at the fragile emitter apex. This way, the contact surface between the electrode and the liquid could be significantly increased, thus eliminating electrochemistry as a serious lifetime limitation.

A more expeditious and potentially severe emitter degradation process involves liquid instabilities on the emitter surface triggered by trapped gases. Such instabilities create conditions favoring electrical discharges,[25,26] leaving decomposed, partially solidified traces between the emitter and extractor, ultimately resulting in electrical shorts, typically in the time frame of minutes to hours of thruster operation. Propellant loading in vacuum or a permeable atmosphere has been implemented to avoid such gas enclosures.[26,8]

Incorporating these findings has allowed for operation under stable emission currents without rapid emitter degradation, thus allowing the study of the behavior of electrospray thrusters over much longer operational times than previously achieved.[8] The work presented here explores the emission characteristics of electrospray thrusters firing for more than 100 hours when integrated with propellant reservoirs that passively feed ionic liquid to the emitter tips. In order to retain the advantage of compactness, these reservoirs are designed to be as small as possible and are qualified for their use in space applications. To the authors' knowledge, this is the first report of such systems where full propellant exhaustion has been demonstrated.

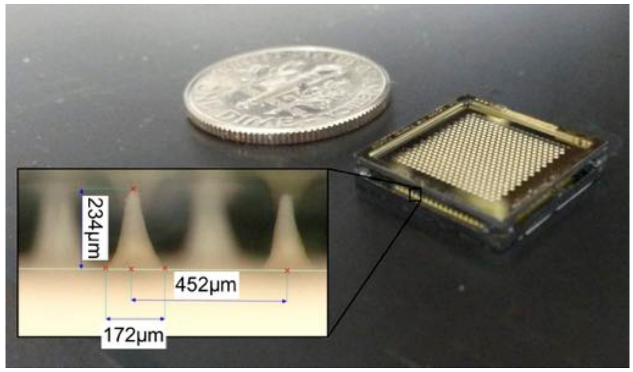

Figure 1. Micromachined electrospray emitter array next to a US Dime coin to scale, and close-up of individual emitter tips

II. Electrospray thruster and reservoir concepts

The thrusters used for this study are MEMS-packaged devices developed at the Space Propulsion Laboratory of the Massachusetts Institute of Technology.[22,8,9] These emitter arrays are based on a porous glass substrate with 480 laser-ablated emitter tips. Emitter-to-extractor electrode alignment is accomplished using a silicon frame structure. The propellant used in this study is 1-ethyl-3-methylimidazolium tetrafluoroborate (EMI-BF_4, Iolitec, $> 98\%$), which is fed to the backside of the emitter substrate through a port in the silicon frame. Fig. 1 shows an emitter array bonded to the extractor grid with individual apertures, as well as an optical microscope image of emitter tips of the array. The thruster package is attached to an ionic liquid reservoir. The specific impulse at voltages ~ 1 kV between the distal electrode and the extractor is $I_{sp} \sim 760$ s with an emission current of $\sim 150\ \mu$A, corresponding to a thrust of $\sim 12.5\ \mu$N per emitter array.[10] At standard room temperature, the EMI-BF_4 propellant has a density of 1.24 g/cm^3, a viscosity of 37 mPa, conductivity of 1.2 S/m at room temperature (22 °C)[27] and surface tension of 44.3 mN/m (22-25 °C).[28]

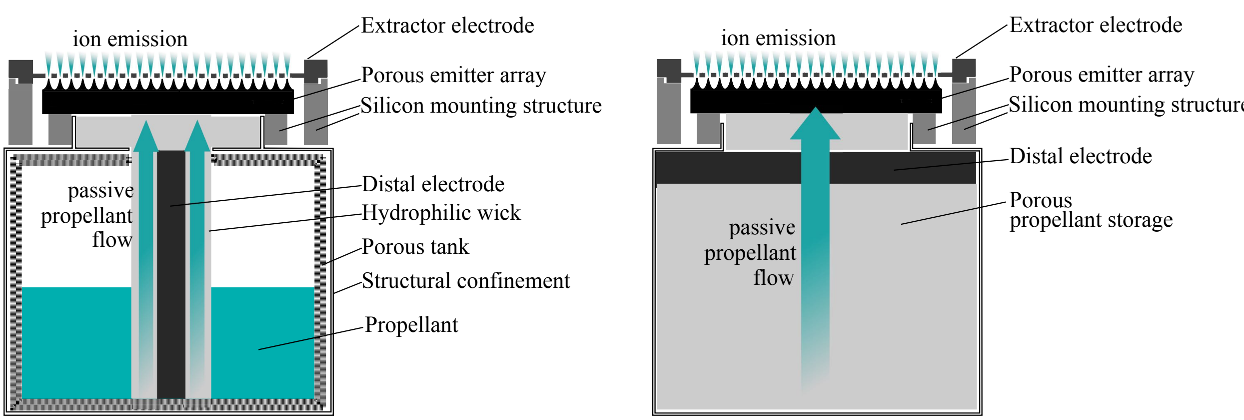

(a) Void volume reservoir (Type I)　　(b) Porous volume reservoir (Type II)

Figure 2. Passive-feeding reservoirs for electrospray thrusters.

The reservoir developed for this study (Type I) features a void volume for propellant storage and includes a IL-philic polyester/glass fiber wick that transports the ionic liquid to the emitter and surrounds the distal electrode, as shown in Fig. 2(a). Propellant is confined inside the reservoir while still allowing system degassing and pressure equalization with the environment by using IL-phobic porous walls. This ensures continuous contact of the propellant with the extraction wick material. Neglecting gravity, propellant flow should be independent from filling level in this configuration, until all liquid stored in the void volume is consumed.

To determine the influence of the propellant reservoir design on emission current, a different, but also unpressurized reservoir concept has been tested, shown in Fig 2(b). In this configuration (Type II), the reservoir is filled with a porous wick material with pore sizes larger than that of the emitter. Glass microfiber is inserted between the wick and the emitter glass substrate to allow passive propellant flow from one to the other. Since the liquid is stored in a porous medium, a dependency of propellant flow from this reservoir on the degree of wick saturation is expected.[29] A small IL-phobic porous membrane is also used in this reservoir to allow gases to escape during pump down, while confining the liquid propellant.

These propellant reservoirs are shown in Fig. 3. The electrospray thrusters used in both are identical except for minor variations due to manufacturing tolerances of the laser-ablated tips on the glass substrate. The thrusters are compact enough to allow placing multiple thrusters on a Cubesat-sized PCB. Propulsion modules featuring 8 or 12 thrusters have been developed. Including PPU, such a module will fit into a 0.5U Cubesat envelope, allowing for two axis attitude control, as well as orbit control.

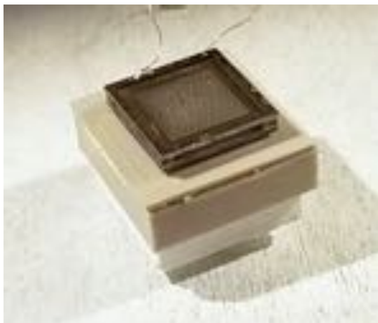

(a) Type I void volume reservoir

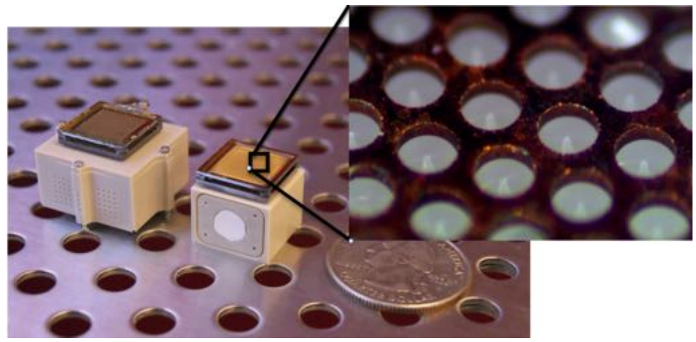

(b) Type II porous volume reservoir (right) and flight-ready Type I reservoir (left)

Figure 3. Propellant reservoirs used in this study. Also shown is a detail of individual emitter tips aligned to extractor apertures.

III. Experimental procedures

Tests were conducted in a ~ 38 liter vacuum chamber with a pumping capacity of 430l/s (N_2) at base pressures $< 5 \times 10^{-6}$ torr when thrusters were idle. Voltage to the distal electrode with respect to the extractor aperture was provided by a Matsusada AP-3B1-L2 laboratory power supply set to alternate the polarity in a trapezoidal wave pattern with a period of 30 s and raise/fall time of 0.5 s. The most relevant measurements in this study are the electric current produced by the emitter array and the current intercepted by the extractor aperture. It is desirable for the intercepted current to be zero at all times to avoid thruster damage. However, due to manufacturing variations at the micro scale, a small fraction (less than 5%) of the emitter current is usually observed. Nevertheless, the intercepted current provides a valuable health monitoring reference, where steady creep to higher values or occasional spikes indicate thruster deterioration. Both the emitted and intercepted currents were measured with an accuracy of ± 0.1 μA, while the emitter voltage monitor reports with an uncertainty of ± 1 V. Thrusters were weighed using an Adam Equipment AAA Series balance (accuracy: 0.1mg). This allows to accurately determine the amount of propellant in the tank and the total mass consumption after the test. In addition, the combination of the integral of the current measurement over time with the consumed propellant mass provides an estimate of the charge to mass ratio of the emitted particles, a critical parameter that helps determine thruster performance.[9,10] Type I thrusters were tested with the emitter array facing up to avoid any asymmetry in the tank due to gravity forces and ensure continuous contact of the liquid with the central wick.

The influence of hydrostatic conditions has been studied by varying the orientation of thrusters with respect to the gravity vector during firing. For constant applied emitter potential, a fully loaded Type I thruster showed 22.9% increase in emitted current when pointing towards gravity, compared to the emitted current when facing up (against gravity). The same thruster, but with significantly emptied propellant reservoir (10-20% fill level, feed wick entirely wetted), showed 22.6% increase in current when facing down. To verify that this increase was primarily caused by hydrostatics related to the propellant supply wick, the tests were repeated with an emitter without tank, where a small amount of propellant was supplied directly to the emitter through a piece of microfiber glass touching the back of the emitter. This emitter showed an increase of only $\sim 3\%$ of emitted current when facing towards gravity, compared to the emission current when emitting against gravity.

IV. Experimental Results

IV.A. Testing of reservoir concepts

Electrospray array emitters show a conditioning phase after first startup in which higher emission potentials are required to achieve a given emission current, most likely attributed to the gradual activation of individual tips in the porous emitter array.[8] After this initial phase, typically lasting less than one hour, emission current stabilizes and its response can be characterized by recording emitted and intercepted currents as a function of emitter potential. This is done for both reservoir types with results shown in Fig. 4(a). The degree of similarity of the two measurements show the negligible impact of propellant reservoir type in this early stage of operation. The duration of this stage is approximately equal to the time it takes for the propellant stored in the glass emitter itself to be consumed.

After characterizing the current vs voltage response, the trapezoidal polarity alternation scheme is implemented as described in Section III for long duration firings with a period of 30 s. Fig. 4(b) shows a detail of the emitted and intercepted currents for a Type I thruster, as well as the emitter potential during one of these tests. This plot also shows the mid-cycle average of the emitted current, which is displayed in all plots hereafter.

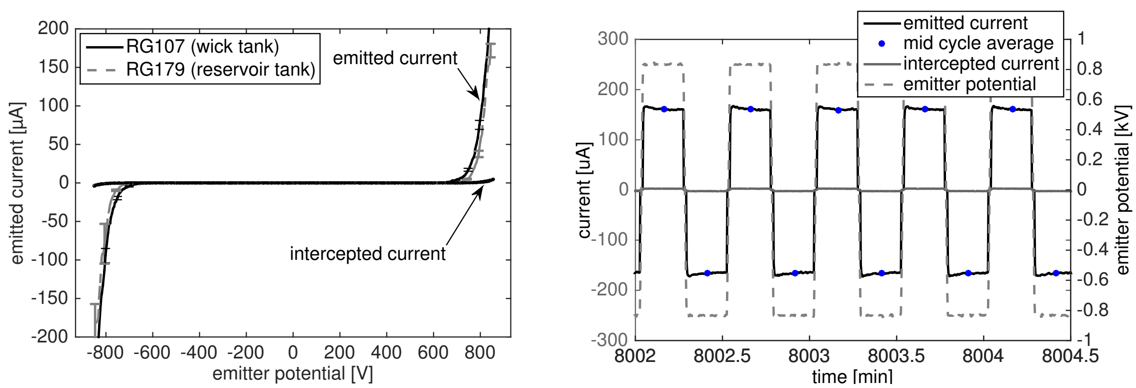

(a) Emitter characterization

(b) Test detail

Figure 4. Emission current as a function of applied voltage and test detail showing applied emitter potential and corresponding emitted and intercepted current traces for a Type I thruster.

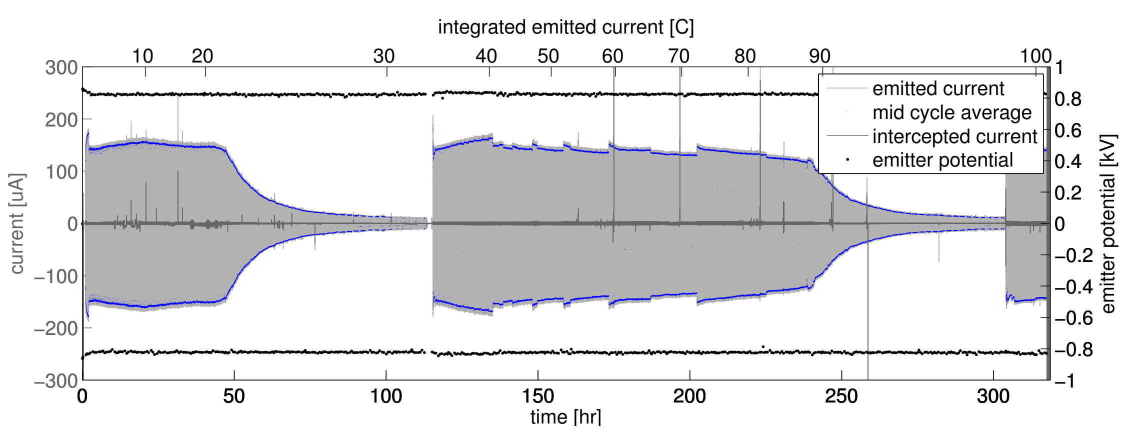

Figure 5. Current traces and applied emitter potential for a refilled Type I thruster.

Fig. 5 summarizes test results from the void volume Type I thruster. The plot shows the (nearly constant) applied emitter potential, and the emitted and intercepted currents as a function of firing time. The total test duration was 317 hr before a short between emitter and extractor forced to end the test. The corresponding accumulated emitted charge is indicated on the top axis to allow comparison against tests with different emission current profiles. This test was started with a reduced reservoir load of 0.8096 g ($\sim$ 43% of the maximum level), to study emission response during reservoir depletion and, while not designed for it, was manually refilled at approximately 115 hr into the test. The refueling procedure involves breaking vacuum, opening the reservoir and injecting fresh propellant. Based on the porosities and geometries of individual reservoir components, about 0.308 g of propellant will be stored in the feed wick, distal electrode and porous glass emitter for this thruster. For the first reservoir refilling, 0.9788 g ($\sim$ 52% of the maximum level) of propellant were loaded to allow for a longer firing time without reservoir depletion. Propellant exhaustion was observed again starting at about 240 hr into the test. A second refilling (1.2557g) was attempted at approximately 300 hr of the test duration, which was only partially successful as the ionic liquid leaked from the emitter surface and produced a short about 17 hr later.

This test displayed relatively stable open-loop emission current largely independent of filling level, up to the point where free liquid in the reservoir is depleted and emission originates from the liquid stored in the wick itself. This is evidenced by an increasingly resistive propellant flow and thus a relatively quick decrease in emission current. After refilling the reservoir, the emission current level is restored to values close to what was obtained prior to the depletion with no change to the emission potential. In the longest continuous firing from 115 hr to approximately 240 hr, a more subtle but steady decrease of emission current is evident, from a maximum of $I \sim \pm 150$ μA at $t = 140$ hr to approximately $I \sim \pm 123$ μA at $t = 240$ hr. The fraction of emitted current that was intercepted by the extractor was measured between 1.1% and 2.3% for positive, and 0.9% and 1.5% for negative emission polarity, with the exception of discharge events.

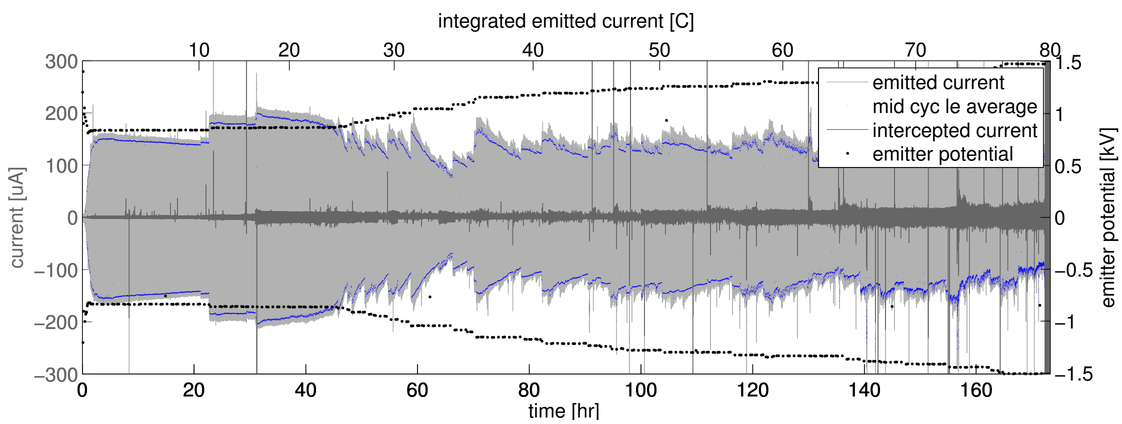

Figure 6. Current traces and applied emitter potential for a porous volume Type II thruster.

Fig. 6 shows the voltage and current traces for an extended duration test of a Type II thruster. The data clearly shows emission current decay at different times, which is compensated for by increasing the emitter voltage. This is very noticeable after approximately 50 hr of firing. Such decay cannot be associated to propellant depletion alone, since a significant amount was still available in the reservoir after this time. During the entire test, a total of 0.6306 g was consumed out of an initial load of 0.9735 g. This shows that the porous volume reservoir was not able to sustain the necessary feed flow. To maintain a relatively constant level of emission current, the emitter potential was continuously raised, leading to increased stressing of the emitter, which is known to favor the occurrence of discharge events. Higher voltages also increases particle interception. Overall, these conditions accelerate the degradation of these devices. This particular test had to be terminated after 172 hr when an electrical short developed between the emitter and the extractor. Throughout the test, relative interception of the emitted current by the extractor grid steadily increased from 1.4% at the beginning of the test to $\sim$ 17% shortly before failure in positive emission polarity, and correspondingly from 1.2% to $\sim$ 12% in negative emission polarity. Note that the intercepted current is a combination of current produced from beam impingement and leakage current caused by decomposed liquid bridging from individual emitters to the apertures.

Fig. 7 shows images of the thrusters after firing. Fig. 7(b) shows the Type I thruster that was refilled and is a composition of the emitter after 300 hr (left) and 317 hr (right). While the emitter displayed a few charred emitter tips after 300 hr of firing, the thruster continued to operate well. The right half of the composition shows the same emitter section after the electrical short occurred. Only 5-7 blocked apertures displaying residue from discharge events could be observed in the emitter, which can be correlated to current surges shown in Fig. 5. While these events induce some degree of degradation, they are not enough to make the device fail. Instead, the definite short came from ionic liquid bridging the gap between the emitter and the extractor. This can be observed in the right frame of Fig. 7(b) and was likely induced after the last refilling attempt.

Fig. 7(a) shows the condition of the Type II thruster after 172 hr. The emitter clearly exhibits signs of increased wear, showing evidence of a large number of discharge events, randomly distributed across the emitter surface. Note that the total integrated emission current was larger for the Type I thruster shown in Fig. 7(b) than for the Type II thruster of Fig. 7(a).

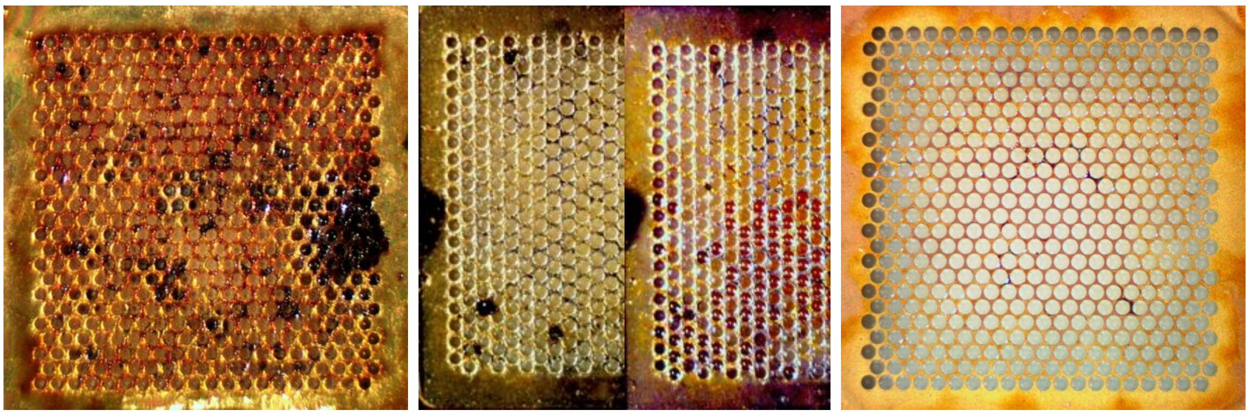

Figure 7. State of thrusters with different reservoirs after firing: (a) Type II after 172 hr, (b) Type I after 300 hr (l) and 317 hr (r), and (c) flight-ready Type I after complete propellant depletion (1 g of propellant in 360 hr).

IV.B. Testing a flight-ready Type I thruster

Based on these findings, a flight-ready Type I thruster as shown in Fig. 3(b) (left) was developed, capable of loading ~ 1 mL of propellant, but filled to a level of approximately 95%. No propellant refilling was attempted for this thruster since the objective was to determine the propellant consumption characteristics under conditions as similar as possible to space. This thruster type underwent a series of environmental tests, including vibration, thermal cycling, vacuum, and centrifugation. Vibration testing was conducted at 21Grms for 60 s in each thruster orientation (according to ULA Atlas V aft bulkhead carrier spectrum[30]), followed by visual inspection and verification of electrical isolation between emitter and extractor. Centrifugation tests were conducted by applying static accelerations of up to 12G, in all orientations, including the emitter tips facing outwards. The thruster was placed in the same vacuum facility as in the tests described above, with the emission direction facing upwards, and was operated using the same laboratory power supply. Fig. 8 shows the voltage, and emitted and intercepted current traces. The recorded data shows stable emission at > 150 μA for the first 125 hr of operation before the free liquid stored in the propellant reservoir was depleted. The thruster was then operated at constant voltage for a total of 362 hr until the net emitted current decreased to $\sim 1\%$ of its initial value and therefore validated the ability to deplete the entire accessible liquid without premature termination due to electrical shorts of other failures.

During the test, a small (~ 500 μm long) fiber fell into one of the extractor apertures and contacted the emitter array at approximately 37 hr into the test, soaking up ionic liquid and producing a small leakage current of 6.5 μA. After the test, the fiber was removed and the corresponding increase of impedance from emitter to extractor was verified. For clarity, this leakage current was subtracted (for > 37 hr) from the emitted and intercepted currents displayed in Fig. 8.

The recorded data displays an overshoot in emission current after polarity alternation, as shown in the inset. The peak value of the overshoot increased with time, as can be seen in Fig. 8. The reason behind this increase is not well understood, although it is likely related to changes in the effective contact area between the distal electrode and the liquid during the formation and depletion of the electrochemical double layer as liquid is consumed. More research is needed to determine the exact nature of this change. Nevertheless, the mid-cycle average remains nearly constant until the onset of propellant exhaustion. Interestingly, the overshoot all but disappears during the current decay. In this test, 1.0139 g of propellant were consumed, out of an initial loading of 1.3168 g. During the test, relative interception increased from 1.4% to 2.7% in positive and from 1% to 2% in negative emission polarity.

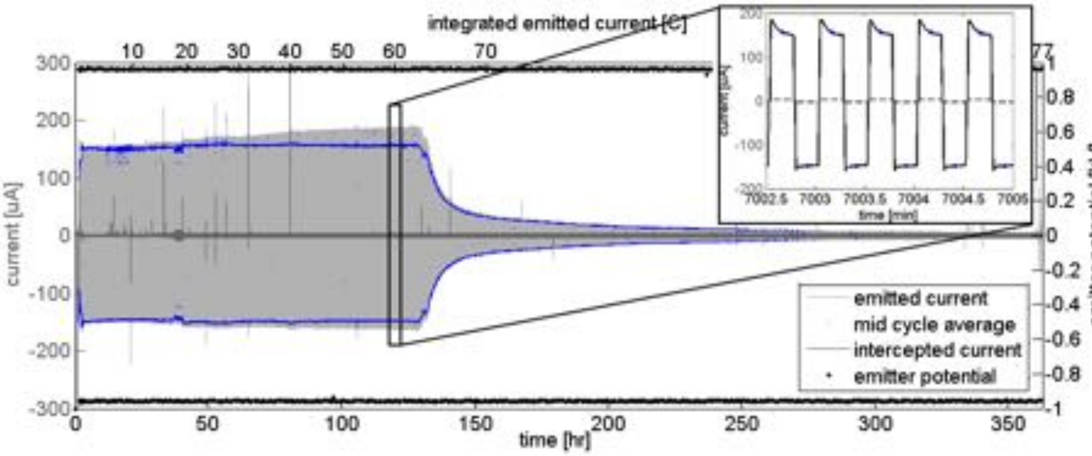

Figure 8. Current traces and applied emitter potential for the flight-ready Type I thruster.

Fig. 7(c) shows the state of the flight-ready Type I thruster after complete propellant depletion. In contrast with the other thrusters, no electrical shorts between emitter and extractor were detected and the emitter face showed no signs of discharges or other indications of thruster degradation.

IV.C. Integrated testing using flight-sized Power Processing Unit

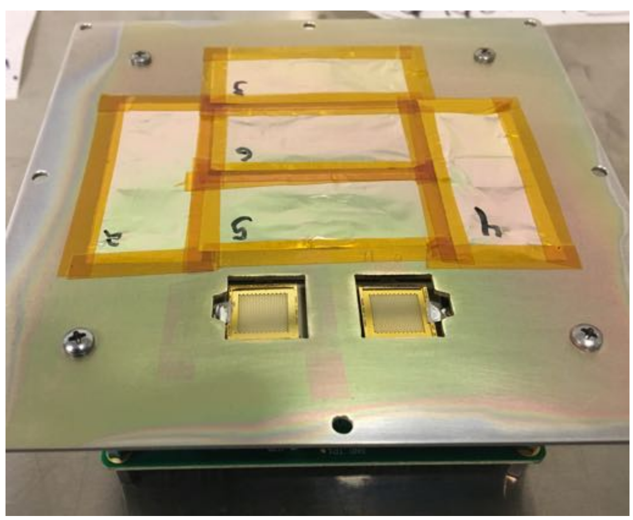

Figure 9. Two type I thrusters integrated to a power processing unit, resistive loads are attached to selected thruster slots. Total propulsion system size is less than 0.5U.

To test thrusters in an environment similar to a flight test, two type I thrusters with approximately half propellant loading were mounted to a Cubesat compatible power supply. This power processing unit (PPU) consisted of two independent power supplies, supplying positive and negative high voltage, with respect to a common, floating ground. The thrusters were connected to these supplies using a switche-able H-bridge design, that allowed each thurster to be connected to either the positive or the negative supply. The extractors of each thruster were connected to a common bias voltage of ~ -25V to repel negative ambient charges. When operating the thursters, the H-bridge design ensured that the thrusters were connected to opposing polarities, and polarity reversal was accomplished by switching the H-bridge. Switch intervals of 30s were used in this test to avoid propellant degradation in the thruster reservoirs. For testing, the PPU and thrusters were enclosed in an aluminum box with cutouts for the thrusters only, to shield the PPU from charged particles. The propulsion unit before mounting in the test enclosure is shown in Fig. 9.

The PPU and thrusters were placed in a $\sim$ 100L vacuum chamber with a pumping capacity of 685l/s (N_2), and a base pressure of $< 5 \times 10^{-7}$torr without thruster operation.

Fig. 10 shows selected telemetry data recorded by the PPU, including the voltage setpoints and selected current readings *Ipos* and *Ineg*, which correspond to the currents drawn from the power supplies measured at the high voltage side. As this measurement location is before the thruster switching circuitry, the data in this plot does not distinguish whether thruster A or B were connected to positive or negative supply. The plot also shows the intercepted currents *intercepted A* and *intercepted B*, which are associated to the thrusters A and B. It should be noted that the intercepted current B is not associated with the negative voltage supply, but is the current intercepted in thruster B independent of applied voltage polarity, and is plotted as negative current only to allow distinction from intercepted current A.

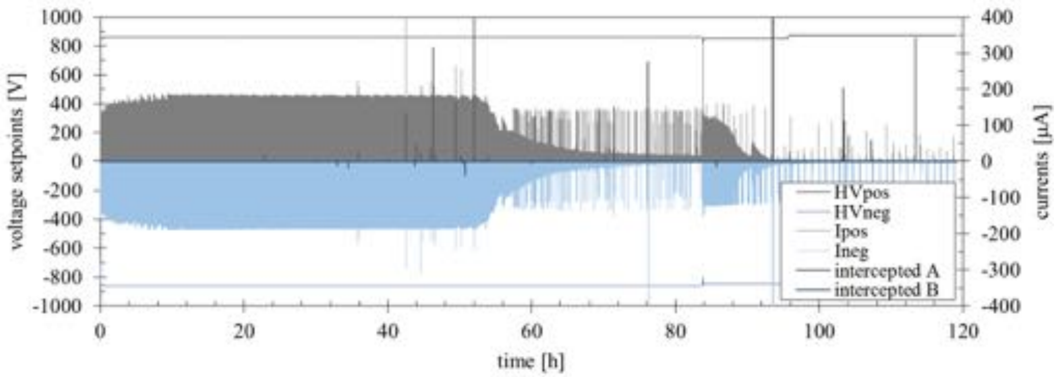

Figure 10. Current traces and voltage setpoints for two flight-ready Type I thruster tested on Cubesat-compatible PPU.

The data recorded shows very stable emission behavior up to $\sim$ 55h of firing. The thrusters were operated in open-loop control slightly above the nominal emission current of 150μA per thruster. The test also validated the ability of a flight-ready Cubesat-sized PPU to start and condition[8] the thrusters. Throughout the test, the thrusters were operated at moderate $\pm$830V.

At $\sim$ 55h, thruster A started to deplete the stored propellant, and emission current started to decay. The design of the PPU with a floating HV ground tends to equalize the currents emitted per polarity to avoid spacecraft charging[19] by allowing a certain shift of the floating supply ground, effectively increasing the emission potential at the thruster which exhibits degrading emission behavior, and corresponding decrease on the other thruster. The thrusters were operated in this mode until $\sim$ 83h into the test, at which point the average emission currents were $< 5\%$ of the nominal emission current during stable operation. From this point forward, the floating power supply was commanded to ground the supplies to allow depletion of the remaining liquid in thruster B. The emission current corresponding to this thruster is clearly noticeable between $83 - 91$h, again with clear signs of propellant depletion. After the emission current had again decreased substantially, the applied voltage was increased to facilitate depletion of any remaining propellant until the test was stopped after a total of 120 hours.

After completion of the test, the thrusters were removed from the chamber and PPU and gravimetric measurements confirmed the depletion of all free liquid in thrusters. Optical and electrical inspection validated that both thrusters were good condition in after the test, with no signs of electrical short or indications of other failures. Fig. 11 shows the emitter arrays of the two thrusters after testing and complete propellant depletion.

V. Discussion

V.A. Propellant consumption characteristics and thruster performance estimation

The data for the Type I thruster in Fig. 5 shows stable emission currents for adequate propellant feed supply at constant applied potential. As soon as free liquid in the reservoir is depleted, feed flow decreases, and a corresponding decrease in emission current is observed. After refilling the reservoir, the current recovers

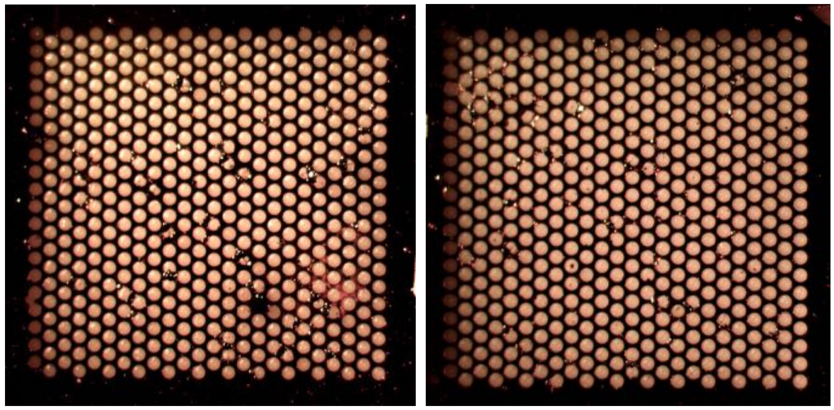

Figure 11. State of thrusters after full propellant depletion, operated by Cubesat-sized PPU

to its original value demonstrating that current decay is associated with the depletion of propellant in the reservoir. Recall these devices were not designed to be refilled, although much was learned from the procedure. Two refills were attempted with the second only partially successful, since the thruster developed a short 17 hr after. However, the emission characteristics changed after the first refill as the current signature developed a series of up and down "steps" in addition to the slow decay described in the previous section. This suggests that the flow was partially enhanced and curtailed, possibly because of changes introduced in the flow path of the propellant management system during the refill. The fact that the first firing prior to the refill does not show these effects reinforces this notion.

This behavior can be compared with the emission current profile from a Type II thruster, in which propellant feed depends on the filling level. In this case, shown in Fig. 6, the continuous current decay required a corresponding increase in applied potential to prevent the emitted current from falling while still having enough propellant in the reservoir. This is to be expected, as in a porous volume reservoir, the propellant feed flow decreases with propellant depletion. This is analogous to the decay stage in Type I thrusters, when the propellant left in the reservoir is exclusively stored in the porous wick. The time of initial stable emission ($\sim$ 44.5 hr) is longer than the expected time to deplete the propellant stored in the porous emitter chip and the glass fiber layers contacting the porous volume reservoir. It is therefore presumed that the storage wick was initially oversaturated, and this excess liquid was readily available for emission. The increased emission potential facilitated the occurrence of discharge events in Fig. 6 that, as mentioned before, eventually led to device shorting.

For the Type I thruster in Fig. 5, no such increase in applied potential was necessary to maintain current levels, and only 5 to 7 discrete discharge events were observed. The number of these events agrees well with the number of charred emitter tips. The corresponding apertures were partially obstructed with signs of decomposed ionic liquid, as shown in Fig. 7(b). These discharge events are more likely to occur in emitter tips with locally increased emission current, as observed by Guerra et al.[31] It is hypothesized that these local events are caused by inhomogeneities in the sintered glass material, given its broad distribution of pore and particle sizes. Interestingly, the appearance of damaged, and in some cases entirely destructed individual emitter tips in an otherwise stable device, shows the ability of these emitter arrays to survive despite such events. Unless their number is relatively large and clustered in a particular location, it appears that the only detrimental effect is a reduction in the overall emission current due to the inability of damaged tips to produce emission.

The results obtained from a flight-ready Type I thruster show that the device was able to fully deplete the reservoir without emission current decay other than that caused by propellant exhaustion (Fig. 8). Visual inspection of the emitter array after firing (Fig. 7(c)) showed no signs of damage, suggesting that longer firing times would have been possible if more propellant volume were provided. While the mid-cycle average in this test showed stable emission up to the point where propellant depletion was noticeable, the recorded data shows a slowly increasing emission current overshoot after polarity alternation. The slow dynamics of this signal, its repeatability, asymmetry in polarity, and absence from the intercepted current trace, suggest that this could be related to electrochemical processes at the distal electrode.

The specific charge of the emitted beam can be determined by the amount of expelled mass and the integrated emitted current. Unfortunately, there are no intermediate mass measurements before current decay happened, which potentially introduces a change in emission properties. Therefore the average specific charge likely overestimates the performance of thrusters before the decay happened, since the reduced flow favors the emission of less massive ionic species over heavier nano-droplets. Taking the average value over the whole duration of the tests result in $q/m \approx 66$ C/g and $q/m \approx 76$ C/g for the refilled and the flight-ready Type I thrusters, respectively. This is not far from the specific charge $q/m \approx 72$ C/g previously measured for Type II thrusters.[10]

The average q/m values allow to estimate the thrust generated by the devices, as well as the total impulse delivered during the tests. However, it was shown in Ref.[10] that the nature of the beam emitted by the array is subject to a variety of losses, including beam spreading and energy inefficiency. The total thruster efficiency of similar electrospray emitters was determined as $\eta = 0.361 \pm 0.081$.[10] The true thrust produced can be calculated according to

$$T = \sqrt{\eta} I \sqrt{2V\frac{m}{q}} \tag{1}$$

For an emission current of $I = 150\mu$A, the thrust produced by the refilled Type I thruster and the flight-ready thruster becomes $T_{refilled} = 14.25 \pm 0.67\mu$N and $T_{flight-ready} = 14.36 \pm 0.68\mu$N at operational potentials of $V_{refill} = 825$V and $V_{flight-ready} = 970$V respectively. This compares reasonably well to previous results of experimental thrust measurements of Type II thrusters, generating $T \sim 11 - 12.5\mu$N at the same emission current.[10] Integrating the thrust as a function of the emitted current over the entire test duration, assuming constant q/m, yields the total impulse produced by the thrusters during the tests. The total impulse delivered by the refilled Type I thruster is determined as $J_{refill} = 9.72 \pm 0.46$ Ns and $J_{flight-ready} = 6.86 \pm 0.33$ Ns for the flight-ready thruster.

V.B. Integrated propulsion module testing

The ability of firing a pair of thrusters using a Cubesat-compatible power processing unit was verified in the test described in Sec. IV.C. In this test, two thrusters were operated in a mode capable of satellite charging mitigation,[19] using a PPU design that allows for a floating high voltage supply ground. In this operational mode, any difference in the emission currents between the paired thrusters leads to a shift in effective thruster extraction potentials, equalizing the emission currents and therefore mitigating satellite charging. In this test, both thrusters were able to deplete the propellant stored in the tanks, and no premature failure was found. Post test optical inspection of the emitters showed only minor signs of wear.

After depletion of the propellant in thruster A, the PPU was operated in a different grounding mode, allowing to deplete the propellant remaining in the other thruster. Both operational modes have therefore been verified over multiple hours.

This test shows the ability of a PPU compatible with power, volume and mass requirements of Cubesats to successfully operate thrusters over extended firing durations. While only two thrusters were tested in this experiment, this PPU is capable of accommodating and powering up to 12 thrusters, as shown in Fig. 9

V.C. Application to Cubesats

The miniaturization of the thrusters allows the design of propulsion modules featuring 8 or more thrusters, including power processing unit (PPU) within a 10x10x5cm package or less.[8,9] A propulsion module described in Sec. IV.C allows individual thruster control,[9] with thrusters typically fired in pairs of opposite polarity to prevent shift of satellite potential.[19] This module can be fitted in Cubesat bus, and the total Δv capability can be estimated, based on the total impulse produced by the flight-ready thruster discussed in section V.A. Using a total propellant loading, with thruster average determined from 23 engineering thrusters as 1.351 ± 0.035g per thruster, and assuming that 0.3g of propellant are inaccessible to emission as found for the flight-ready thruster (section IV.B), the total Δv available to a spacecraft can be estimated as function of total spacecraft mass according to the Tsiolkovsky rocket equation. The specific impulse is derived from the measured charge-to-mass ratio of $q/m \approx 76$ C/g and the thruster efficiency reported in Ref.,[10] resulting in I_{sp}=743.7 $\pm$ 83.4s for the flight-ready thruster design. The total Δv capability corresponding to eight fully exhausted thrusters is plotted in Fig. 12 as a function of initial satellite mass. The plot also shows the resulting Δv for a module housing 12 identical thrusters.

The thrust calculated in section V.A allows to determine the torque produced by a pair of thrusters exerted on a Cubesat, in a propulsion module configuration as tested in Sec. IV.C. In this configuration, thruster pairs are symmetrically distributed at a normal distance of 3.36cm from the Cubesat central axis, with the thrust axis facing parallel to the longest satellite dimension. The torque τ exerted by firing a pair of thrusters at emission current of 150μA each is calculated as $\tau = 0.95 \pm 0.05\mu$Nm. The resulting changes in Cubesat rotation rates are shown in Fig. 12 for continuous firing of a pair of thrusters for 1 and 10 minutes at 150μA emission current per thruster, assuming a uniform distribution of spacecraft mass. It should be noted that the thrusters can be continuously throttled as evident from the current/voltage characteristic in Fig. 4(a), allowing, in combination with the overall low thrust level, use as high precision attitude actuators. Such application has been shown in Ref.,[32] where impulse bits as small as 1μNs per thruster and stable attitude control better than 22 arcseconds over 10h were experimentally verified in a laboratory environment.

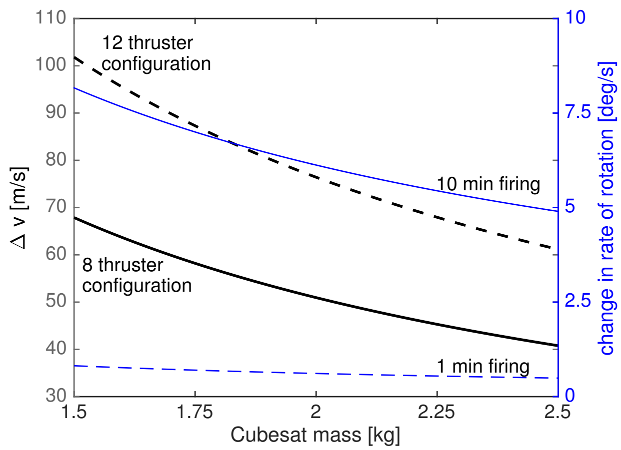

Figure 12. Total Δv for 8 and 12 fully exhausted thrusters, and change in satellite rotation as a function of initial spacecraft mass.

VI. Conclusion

The results of extended firing tests of ionic liquid, MEMS-based electrospray thrusters with two different propellant reservoir systems are presented. The test data show that it is possible to operate these thrusters in open-loop mode for > 100 hr with emission current levels of ~ 150 μA and constant applied potential, without observing fast emission current decay. This is achieved by employing a distal electrode to minimize influence of electrochemistry, and by ensuring stable passive propellant supply from an unpressurized reservoir. It was found that, although not ideal, these thrusters could be refilled and that this procedure recovers the emission characteristics prior to the decay in current level induced by propellant depletion. This work reports the first documented instance of full reservoir depletion from a flight-ready electrospray thruster with ~ 1 mL capacity, which was fired for ~ 130 hr at full throttle before current started to decay. This device was then fired for ~ 350 hr until all propellant accessible for emission was consumed. The thruster produced a thrust of $T = 14.36 \pm 0.68\mu$N at an operational potential of $V = 970$V, corresponding to an emission current of $I = 150\mu$A. Visual inspections after the test showed no signs of damage to this thruster. Two flight-ready thrusters were then tested powered by a Cubesat-sized power processing unit, and both thrusters were able to deplete the stored propellant load without premature failure. Application of this technology to Cubesats as small as 1.5U are discussed, with an 8 thruster module providing a $\Delta v \sim 50$ m/s for a 2kg spacecraft in a 8 thruster configuration, based on experimentally determined performance data.

Acknowledgments

The authors would like to thank Francois Martel, Frank LaRosa and Jerry Roberts for supplying the power processing unit for the integrated propulsion module test, and Fernando Mier-Hicks for his support of the experimental testing. This work was supported by the US Government.

References

[1]H. Heidt, J. Puig-Suari, A. Moore, S. Nakusuka, and R. Twiggs, "Cubesat: A new generation of picosatellite for education and industry low-cost space experimentation," in *Small Satellite Conference*, no. SSC00-V-5, (Logan, UT), 2000.

[2]D. Selva and D. Krejci, "A survey and assessment of the capabilities of cubesats for earth observation," *Acta Astronautica*, vol. 74, pp. 50 – 68, 2012.

[3]M. Swartwout, "The first one hundred cubesats: A statistical look," *Journal of Small Satellites*, vol. 2, no. 2, pp. 213–233, 2013.

[4]P. Lozano and M. Martínez-Sánchez, "Ionic liquid ion sources: suppression of electrochemical reactions using voltage alternation," *Journal of Colloid and Interface Science*, vol. 280, no. 1, pp. 149 – 154, 2004.

[5]P. Lozano and M. Martínez-Sánchez, "Ionic liquid ion sources: Characterization of externally wetted emitters," *Journal of Colloid and Interface Science*, vol. 282, no. 2, pp. 415 – 421, 2005.

[6]R. Krpoun and H. R. Shea, "Integrated out-of-plane nanoelectrospray thruster arrays for spacecraft propulsion," *Journal of Micromechanics and Microengineering*, vol. 19, no. 4, p. 045019, 2009.

[7]D. G. Courtney, H. Q. Li, and P. Lozano, "Emission measurements from planar arrays of porous ionic liquid ion sources," *Journal of Physics D: Applied Physics*, vol. 45, no. 48, p. 485203, 2012.

[8]D. Krejci, F. Mier Hicks, C. Fucetola, P. Lozano, A. Hsu Schouten, and F. Martel, "Design and characterization of a scalable ion electrospray propulsion system," in *34th International Electric Propulsion Conference*, no. IEPC-20150149, (Hyogo-Kobe, Japan), 2015.

[9]D. Krejci and P. Lozano, "Scalable ionic liquid electrospray thrusters for nanosatellites," in *AAS Guidance and Control Conference*, no. AAS 16-124, (Breckenridge, CO), 2016.

[10]D. Krejci, F. Mier-Hicks, R. Thomas, T. Haag, and P. Lozano, "Emission characteristics of passively fed electrospray microthrusters with propellant reservoirs," *Journal of Spacecraft and Rockets*, vol. 54, no. 2, pp. 447–458, 2017.

[11]D. G. Courtney, S. Dandavino, and H. Shea, "Comparing direct and indirect thruster measurements from passively fed and highly ionic electrospray thrusters," *Journal of Propulsion and Power*, vol. 32, no. 2, 2015.

[12]L. B. King, E. Meyer, M. A. Hopkins, B. S. Hawkett, and N. Jain, "Self-assembling array of magnetoelectrostatic jets from the surface of a superparamagnetic ionic liquid," *Langmuir*, vol. 30, no. 47, pp. 14143–14150, 2014. PMID: 25372842.

[13]W. Wright and P. Ferrer, "Electric micropropulsion systems," *Progress in Aerospace Sciences*, vol. 74, pp. 48 – 61, 2015.

[14]G. I. Taylor, "Disintegration of water drops in an electric field," *Proceedings of the Royal Society A*, vol. 280, pp. 383–397, 1964.

[15]P. Lozano and M. Martinez-Sanchez, "Experimental measurements of colloid thruster plumes in the ion-droplet mixed regime," in *38th AIAA/ASME/SAE/ASEE Joint Propulsion Conference & Exhibit*, American Institute of Aeronautics and Astronautics, 2012/04/06 2002.

[16]I. Romero-Sanz, R. Bocanegra, and J. F. de la Mora, "Source of heavy molecular ions based on taylor cones of ionic liquids operating in the pure ion evaporation regime," *Journal of Applied Physics Appl Phys.*, vol. 5, no. 94, pp. 3599–3605, 2003.

[17]D. Garoz, B. C., C. Larriba, S. Castro, I. Romero-Sanz, J. de la Mora, Y. Yoshida, and G. Saito, "Taylor cones of ionic liquids from capillary tubes as sources of pure ions: The role of surface tension and electrical conductivity," *Journal of Applied Physics*, vol. 102, no. 6, 2007.

[18]C. Coffman, M. Martínez-Sánchez, F. J. Higuera, and P. C. Lozano, "Structure of the menisci of leaky dielectric liquids during electrically-assisted evaporation of ions," *Applied Physics Letters*, vol. 109, no. 23, p. 231602, 2016.

[19]F. Mier-Hicks and P. Lozano, "Spacecraft charging characteristics induced by the operation of electrospray thrusters," *Journal of Propulsion and Power*, vol. 33, no. 2, pp. 456–467, 2017.

[20]V. Khayms, *Advanced Propulsion for Microsatellites*. PhD thesis, Massachusetts Institute of Technology. Department of Aeronautics and Astronautics, 2000.

[21]L. E. Perna, F. Mier Hicks, C. S. Coffman, H. Li, and P. C. Lozano, "Progress toward demonstration of remote, autonomous attitude control of a cubesat using ion electrospray propulsion systems," in *48th AIAA/ASME/SAE/ASEE Joint Propulsion Conference & Exhibit*, no. AIAA 2012-4289, (Atlanta, Georgia), 2012.

[22]C. Coffman, L. Perna, H. Li, and P. C. Lozano, "On the manufacturing and emission characteristics of a novel borosilicate electrospray source," in *49th AIAA/ASME/SAE/ASEE Joint Propulsion Conference*, (San Jose, CA), 2013.

[23]R. S. Legge, "Fabrication and characterization of porous metal emitters for electrospray applications," Master's thesis, Massachusetts Institute of Technology. Department of Aeronautics and Astronautics, 2008.

[24]D. G. Courtney, *Ionic Liquid Ion Source Emitter Arrays Fabricated on Bulk Porous Substrates for Spacecraft Propulsion*. PhD thesis, Massachusetts Institute of Technology. Department of Aeronautics and Astronautics, 2011.

[25]N. Brikner and P. C. Lozano, "The role of upstream distal electrodes in mitigating electrochemical degradation of ionic liquid ion sources," *Applied Physics Letters*, vol. 101, no. 19, p. 193504, 2012.

[26]N. Brikner, *On the Identification and Mitigation of Life-Limiting Mechanisms of Ionic Liquid Ion Sources Envisaged for Propulsion of Microspacecraft*. PhD thesis, Massachusetts Institute of Technology. Department of Aeronautics and Astronautics, 2015.

[27]J. Fuller, R. T. Carlin, and R. A. Osteryoung, "The room temperature ionic liquid 1ethyl3methylimidazolium tetrafluoroborate: Electrochemical couples and physical properties," *J. Electrochem. Soc.*, vol. 144, no. 11, pp. 3881–3886, 1997.

[28]W. Martino, J. F. de la Mora, Y. Yoshida, G. Saito, and Wilkes, "Surface tension measurements of highly conducting ionic liquids," *Green Chem.*, vol. 8, pp. 390–397, 2006.

[29]D. G. Courtney and H. Shea, "Influences of porous reservoir laplace pressure on emissions from passively fed ionic liquid electrospray sources," *Applied Physics Letters*, vol. 107, no. 10, 2015.

[30]ULA, *Aft Bulkhead Carrier Auxilliary Payload User's Guide*. United Launch Alliance, May 2014.

[31]C. Guerra-Garcia, D. Krejci, and P. Lozano, "Spatial uniformity of the current emitted by an array of passively fed electrospray porous emitters," *Journal of Physics D: Applied Physics*, vol. 49, no. 11, p. 115503, 2016.

[32]F. Mier-Hicks and P. C. Lozano, "Electrospray thrusters as precise attitude control actuators for small satellites," *Journal of Guidance, Control, and Dynamics*, vol. 40, pp. 642–649, 2017.